A Nearly Exact Discretization Scheme for the FitzHugh-Nagumo Model

Eddy Kwessi* and Lloyd J. Edwards†

Abstract

In this paper, we apply the nearly exact discretization schemes to propose a discrete model for the FitzHugh Nagumo model. We show that the discrete model obtained preserves the dynamics and the known features of the continuous FitzHugh-Nagumo model. We do so by performing distance-based and probability-based similarity analysis. Additionally, a sensitivity analysis is also performed to analyze the most influential parameters of the discrete system.

Keywords: Neurones; FitzHugh-Nagumo; non-standard, discrete model.

AMS Subject Classification: 62J05; 62G08; 62G86; 62F12

1 Introduction

Hodgkin [7] famously were able to use voltage clamping and pharmacology agents to model the ionic conductances that generate the action potential of nerve fibers, see [2]. They proposed a model based on four coupled equations linking the following variables: the membrane potential, the sodium activation current, the sodium inactivation current, and the potassium activation current. The continuous FitzHugh-Nagumo (CFHN) model was independently obtained in [3] and in [17] from the Hodgkin-Huxley (HH) model by considering fast and slow variables and slaving the others. Indeed, the model is justified by the observation that both the membrane potential and the sodium activation current evolve on a similar time scale during an action potential whereas the sodium inactivation current and the potassium activation current change on a much slower time scale. The two coupled variables of the CFHN model are x, called the membrane potential whose role is to reproduce the behavior of the voltage during the course of a spike and y, called the recovery variable whose role is to inhibit the production of x (slow negative feedback), see for instance [10]. There are many variants of the CFHN model, but in this paper we will adopt the model given as

$$\begin{cases} \epsilon \frac{dx}{dt} = x - \frac{x^3}{3} - y + I \\ \frac{dy}{dt} = x + a - \gamma y \end{cases}, \tag{1.1}$$

where a is the excitability parameter of the system in the sense that it determines if the system is excitable or not (that is, it exhibits periodic firing and thus autonomous oscillations), γ is a

*Corresponding author, Department of Mathematics, Trinity University, San Antonio, TX, USA, ekwessi@trinity.edu

†Department of Biostatistics, University of Alabama at Birmingham, Birmingham, AL, USA, ljedward@uab.edu

parameter playing similar role as a and represents an excitation threshold, ϵ is a positive scaling parameter determining how fast x changes relatively to y, and I is the intensity of the injected current and is a constant of time t. We note that with the change of variable $u = x + a$ and $v = \epsilon^{-1}y$, the system (1.2) model is equivalent to the more abstract form (see [10]) given as

$$\begin{cases} \frac{du}{dt} = h(u) - v + I_0 \\ \frac{dv}{dt} = c_1(u - c_2 v) \end{cases}, \tag{1.2}$$

where $c_1 = \epsilon^{-1}, c_2 = \gamma\epsilon, I_0 = \epsilon^{-1}I$ and $h(u)$ is a third degree polynomial in u. The CFHN model is useful not only to model interaction between neural networks, but also to understand the structure of nerve axons in vertebrates [2].

The literature on the dynamics of the system of ordinary differential equations (1.2) is rather large. Discrete versions of this model have been proposed for various reasons: Hupkes and Sandstede [9] considered a discrete FHN model and showed that it possesses traveling pulses. Elmer and Van Vleck [2] discussed a spatially discrete FHN model and compared its dynamics to the dynamics generated by spatially continuous and discrete models of action potential propagation. Jing et al. [11] have proposed a discrete version of the CFHN model using the Euler discretization method and showed that the system they obtained has a chaotic behavior: invariant cycle, period doubling bifurcations, and other properties. Other recent references about the FHN worth looking into and that provide additional details include [4, 12, 13, 19] and the references therein.

Discrete models obtained from continuous models should have at least some of the following properties: preserve the dynamics of the original continuous model, be mathematically tractable, be well-posed, and be practical for parameter estimation. Our contribution in this paper is to propose a discrete Fitzhugh-Nagumo (DFHN) model, based on a nearly exact discretization scheme (NEDS)[14]. We show that the resulting model preserves qualitatively and quantitatively the features of the continuous model such as its dynamics and known phenomena. The remainder of the paper is organized as follows: in Section 2, we provide a brief overview of the NEDS method. In Section 3, we present the FHN model and in Section 4, we establish dynamics and stability of the DFHN model. In Section 5, we present simulations addressing equibria and the preservation of known phenomena to the CFHN model and Section 6 provides a deeper examination of the DFHN model. Lastly, in Section 7, we discuss some concluding remarks.

2 Review of the NEDS Method

We note that the NEDS is one of the many iterations of the methods proposed in [15, 16] that applies to the case where the right hand side of an ordinary differential equation (ODE) has a specific form. Let x be a function of t. The ODE notation of x is $x(t)$ whereas the difference equation (DE) notation for x is x_t. Consider the following:

$$\frac{dx}{dt} = f(x(t)), \tag{2.1}$$

where $f(x)$ is a real-valued function of x.

Definition 1. *A discretization scheme will be called dynamically consistent if the following hold:*

A1: *The stability of the ODE and DE are the same.*

A2: *The bifurcation of the ODE and DE are the same.*

A3: *If two ODEs are equivalent through re-parametrization, then the resulting DEs must be equivalent through the same re-parametrization.*

Definition 2. *A real-valued function f is said to be T_1 if $f(x) = \omega x + g(x)x + c$ and is T_2 if $f(x) = \omega x - g(x)x + c$, where ω is a nonzero real constant, $g(x)$ a real-valued function that has no linear term, and c is a constant function of x.*

A NEDS of the ODE in (2.1) can be obtained using the following principles:

P1: The derivative $\dfrac{dx}{dt}$ can be discretized as

$$\frac{x_{t+1} - x_t}{\phi(\tau)}, \tag{2.2}$$

where ϕ depends on a step size τ and other parameters, and is given as

$$\phi(\tau) \quad = \quad \tau + \mathrm{O}(\tau^2) \quad \text{as } \tau \to 0^+.$$

P2: Suppose f is either T_1 or T_2. We define

$$\phi(\tau) = \frac{e^{\omega\tau} - 1}{\omega}.$$

Thus

$$\frac{x_{t+1} - x_t}{\phi(\tau)} = \begin{cases} \omega x_t + g(x_t)x_t + c\,, & \text{if } f \text{ is } T_1 \\ \\ \omega x_t - g(x_t)x_{t+1} + c\,, & \text{if } f \text{ is } T_2 \end{cases}.$$

In this case the resulting DE is

$$x_{t+1} = f_0(x_t) = \begin{cases} e^{\omega\tau}x_t + \phi(\tau)[g(x_t)x_t + c], & \text{if } f \text{ is } T_1 \\ \\ \frac{e^{\omega\tau}x_t + \phi(\tau)c}{1+\phi(\tau)g(x_t)}, & \text{if } f \text{ is } T_2 \end{cases}. \tag{2.3}$$

This NEDS has been used successfully to obtain dynamically consistent DE models from various types of nonlinear model ODEs that cannot be linearized, see for instance [14] and [6] .

3 NEDS for the FitzHugh-Nagumo Model

Now let us rewrite the CFHN model (1.2) above as:

$$\begin{cases} \dfrac{dx}{dt} = \epsilon^{-1}x - \epsilon^{-1}\dfrac{x^3}{3} - \epsilon^{-1}y + \epsilon^{-1}I \\ \dfrac{dy}{dt} = x + a - \gamma y \end{cases}. \tag{3.1}$$

Let

$$\phi_1(\tau) = \frac{e^{\epsilon^{-1}\tau} - 1}{\epsilon^{-1}} \text{ and } \phi_2(\tau) = \frac{1 - e^{-\gamma\tau}}{\gamma}\,.$$

Letting $g_1(x) = \epsilon^{-1}\dfrac{x^2}{3}$ and $g_2(y) = 0$, we observe that (3.1) can be written in the form

$$\begin{cases} \dfrac{dx}{dt} = \epsilon^{-1}x - g_1(x)x + \epsilon^{-1}(I - y) \\ \dfrac{dy}{dt} = -\gamma y + g_2(y)y + x + a \end{cases} . \tag{3.2}$$

Using $\phi_1(\tau)$ to discretize the first equation and $\phi_2(\tau)$ to discretize the second equation in (3.2), the NEDS method as suggested above yields the following:

$$\begin{cases} x_{t+1} = f_0(x_t, y_t, \epsilon, \tau, I) = \dfrac{e^{\epsilon^{-1}\tau}x_t + (1 - e^{\epsilon^{-1}\tau})(y_t - I)}{1 + \dfrac{e^{\epsilon^{-1}\tau} - 1}{3}x_t^2} \\ y_{t+1} = h_0(x_t, y_t, \gamma, \tau, a) = e^{-\gamma\tau}y_t + \gamma^{-1}(1 - e^{-\gamma\tau})(x_t + a) \end{cases} . \tag{3.3}$$

For simplification purposes, we may sometimes use the re-parametrization

$$\alpha = e^{\epsilon^{-1}\tau}, \quad \beta = e^{-\gamma\tau}, \text{ and } \theta = \gamma^{-1} ,$$

so that (3.3) may we written as

$$\begin{cases} x_{t+1} = f(x_t, y_t, \alpha, I) = \dfrac{\alpha x_t + (1 - \alpha)(y_t - I)}{1 + \dfrac{\alpha - 1}{3}x_t^2} \\ y_{t+1} = h(x_t, y_t, \beta, \theta, a) = \beta y_t + \theta(1 - \beta)(x_t + a) \end{cases} . \tag{3.4}$$

In the next sections, we show that the dynamics of the discrete FHN is nearly identical to the dynamics of the continuous one. Henceforth, CFHN will denote either equations (1.2), (3.1), or (3.2) whereas DFHN will denote either (3.3) or (3.4). We start by comparing the times series of CFHN and that of the DFHN.

4 Dynamics of the DFHN model

4.1 Fixed points

The fixed points of the DFHN model are solutions of the equations $x_{t+1} = x_t$ and $y_{t+1} = x_t$. Therefore

$$x_{t+1} = x_t \iff \alpha x_t + (1 - \alpha)(y_t - I) = x_t + \frac{\alpha - 1}{3}x_t^3 .$$

Thus,

$$y_t = x_t - \frac{x_t^3}{3} + I. \tag{4.1}$$

Likewise,

$$y_{t+1} = x_t \iff y_t = \beta y_t + \theta(1 - \beta)(x_t + a) .$$

Thus,

$$y_t = \theta(x_t + a). \tag{4.2}$$

We note that equations (4.1) and (4.2) represent respectively the nullclines (or isoclines) of x and y in the CFHN model, that is, where the velocities $\dfrac{dx}{dt} = 0$ and $\dfrac{dy}{dt} = 0$. Therefore, we conclude that the continuous and discrete models have the same nullclines or same fixed points.

Dropping the reference to t and combining equations (4.1) and (4.2), we obtain:

$$x^3 + px + q = 0, \tag{4.3}$$

where $p = -3\left(1 - \frac{1}{\gamma}\right)$ and $q = -3\left(I - \frac{a}{\gamma}\right)$. The discriminant of equation (4.3) is given as

$$\Delta = \Delta(a, \gamma, I) = 27\left[4\left(1 - \frac{1}{\gamma}\right)^3 - 9\left(I - \frac{a}{\gamma}\right)^2\right].$$

We know that:

(a) If $\Delta < 0$, then there is one real root and two complex conjugate roots with nonzero imaginary parts.

(b) If $\Delta = 0$, then there is one real root and one root of multiplicity 2.

(c) If $\Delta > 0$, then there are three distinct real roots.

4.2 Stability Analysis

To discuss stability analysis of a two-dimensional discrete system, we recall the following result, Theorem 4.11 in [1].

Theorem 3. *Let $F : G \subset \mathbb{R}^2 \to \mathbb{R}^2$ be a continuously differentiable map, where G is an open set of $\mathbb{R}^2$. Let $\mathbf{X}$ be a fixed point of F, and let $\mathbf{A} = JF(\mathbf{X})$, where $JF(\mathbf{X})$ is the Jacobian of F evaluated at $\mathbf{X}$. Let $\sigma(\mathbf{A}) = \max\{|\lambda_1|, |\lambda_2|\}$ be the spectral radius of $\mathbf{A}$, where λ_i, $i = 1, 2$ is an eigen value of $\mathbf{A}$. Then the following statements hold true:*

- *If $\sigma(\mathbf{A}) < 1$, then $\mathbf{X}$ is asymptotically stable.*
- *If $\sigma(\mathbf{A}) > 1$, then $\mathbf{X}$ is unstable.*
- *If $\sigma(\mathbf{A}) = 1$, then $\mathbf{X}$ may or may not be stable.*

Remark 4. *We observe that if $\mathbf{A}$ is 2×2 matrix, then $\sigma(\mathbf{A}) < 1$ if and only if $|tr(\mathbf{A})| - 1 < det(\mathbf{A}) < 1$. This is the so-called Trace-Determinant Theorem, see [1].*

Consider the two dimensional map $F : \mathbb{R}^2 \to \mathbb{R}^2$ defined as

$$F(x, y) = \begin{cases} f(x, y) = \dfrac{\alpha x + (1 - \alpha)(y - I)}{1 + \dfrac{\alpha - 1}{3}x^2} \\ \\ g(x, y) = \theta(1 - \beta)(x + a) + \beta y \end{cases}.$$

Clearly, F is continuously differentiable on $\mathbb{R}^2$. Let $\mathbf{X} = (x, y)$ be a fixed point of the DFHN. The Jacobian $\mathbf{A} = JF(\mathbf{X})$ of F is given as

$$JF(\mathbf{X}) = \begin{pmatrix} \dfrac{3\alpha + (\alpha - 1)x^3 - 2(\alpha - 1)x[\alpha x + (1 - \alpha)(y - I)]}{3\left(1 + \dfrac{\alpha - 1}{3}x^2\right)^2} & \dfrac{(1 - \alpha)}{1 + \dfrac{\alpha - 1}{3}x^2} \\ \theta(1 - \beta) & \beta \end{pmatrix}.$$

Replacing y in the Jacobian with $\theta(x+a)$, and simplifying, we have

$$JF(\mathbf{X}) = \begin{pmatrix} \dfrac{L}{3K^2} & \dfrac{(1-\alpha)}{K} \\ \theta(1-\beta) & \beta \end{pmatrix} ,$$

where

$$L = L(x) = (\alpha-1)\mu_1 x^2 + \mu_2 x + 3\alpha \quad \text{and } K = K(x) := 1 + \frac{\alpha-1}{3}x^2 ,$$

with $\mu_1 = 2\theta - \alpha(1+\theta)$ and $\mu_2 = 2(\alpha-1)^2(\theta a - I)$. Consider the following quantities that will be crucial for stability analysis:

$$\begin{aligned} T &= tr(\mathbf{A}) = \beta + \frac{L}{3K^2}; \quad D = det(\mathbf{A}) = \frac{\beta L}{3K^2} + \frac{\lambda}{K} . \\ \lambda &= \theta(1-\beta)(\alpha-1) \end{aligned}$$

From Remark 4, $D < 1$ if $P_0(K) = 3K^2 - 3\lambda K - \beta L > 0$ for all K. We observe that $\alpha > 1$ so that $K > 0$ for all $x \in \mathbb{R}$. $P_0(K)$ is a second degree polynomial in K with positive leading coefficient, therefore it is positive for all K if $(\boldsymbol{A_{1,\beta}})$: $\Delta_\beta = 9\lambda^2 + 12\beta L < 0$ and $(\boldsymbol{A_{2,\beta}}) : P_0(C_0) = -\frac{3}{4}\lambda^2 - \beta L > 0$.

$(\boldsymbol{A_{2,\beta}})$ suggests that the critical point $C_0 = \frac{1}{2}\lambda$ is such that $P_0(C_0) = -\frac{3}{4}\lambda^2 - \beta L > 0$, otherwise, there will be values of K for which $P_0(K) < 0$.
Let us examine $(\boldsymbol{A_{1,\beta}})$.
$\Delta_\beta < 0 \iff P_1(x) = 12\beta(\alpha-1)\mu_1 x^2 + 12\beta\mu_2 x + 36\alpha\beta + 9\lambda^2 < 0$. Let $C_{1,\beta} = \dfrac{-\mu_2\beta}{2\beta(\alpha-1)\mu_1}$ be the critical point of $P_1(x)$. Then $(\boldsymbol{A_{1,\beta}})$ is possible for all x if

$$(\boldsymbol{A_{1,1,\beta}}) : \begin{cases} \mu_1 < 0, \\ \Delta_{1,\beta} = 144\beta^2\mu_2^2 - 48\mu_1\beta(\alpha-1)[36\alpha\beta + 9\lambda^2] < 0 \\ P_1(C_{1,\beta}) < 0 \end{cases} ,$$

or for some x if

$$(\boldsymbol{A_{1,2,\beta}}) : \begin{cases} \mu_1 > 0, \\ \Delta_{1,\beta} = 144\beta^2\mu_2^2 - 48\mu_1\beta(\alpha-1)[36\alpha\beta + 9\lambda^2] > 0 \\ P_1(C_{1,\beta}) < 0 \end{cases} .$$

We observe that $\mu_1 < 0$ makes $\Delta_{1,\beta} > 0$ in $(\boldsymbol{A_{1,1,\beta}})$, therefore only $(\boldsymbol{A_{1,2,\beta}})$ is possible.
Let us examine $(\boldsymbol{A_{2,\beta}})$.
$P_0(C_0) > 0 \iff P_2(x) = -\beta(\alpha-1)\mu_1 x^2 - \mu_2\beta x - \left[3\alpha\beta + \frac{3}{4}\lambda^2\right] > 0$. $C_{2,\beta}$ is the critical point of $P_2(x)$ given by $C_{2,\beta} = C_{1,\beta}$. The inequality is only possible for all x if

$$(\boldsymbol{A_{2,1,\beta}}) : \begin{cases} \mu_1 > 0 \\ \Delta_{2,\beta} = \beta^2\mu_2^2 - 4\beta(\alpha-1)\mu_1\left[3\alpha\beta + \frac{3}{4}\lambda^2\right] < 0 \\ P_2(C_{2,\beta}) < 0 \end{cases} ,$$

or for some x if

$$(\boldsymbol{A_{2,2,\beta}}) : \begin{cases} \mu_1 < 0 \\ \Delta_{2,\beta} = \beta^2\mu_2^2 - 4\beta(\alpha-1)\mu_1\left[3\alpha\beta + \frac{3}{4}\lambda^2\right] > 0 \\ P_2(C_{2,\beta}) < 0 \end{cases} .$$

Only $(\boldsymbol{A_{2,1,\beta}})$ overlaps with $(\boldsymbol{A_{1,2,\beta}})$, so in conclusion, $D < 1$ if the following conditions (which depend only on the parameters α, β, θ, a, and I) are true:

$$P_1(\beta) = P_1(\alpha, \beta, \theta, a, I) : \begin{cases} \mu_1 > 0 \\ \Delta_{1,\beta} > 0, \quad \Delta_{2,\beta} < 0 \\ P_1(C_{1,\beta}) < 0, \quad P_2(C_{1,\beta}) < 0 \end{cases} .$$

Now, we discuss the conditions for $|T| - 1 < D$.
Case 1: $L > 0$
Then $|T| - 1 - D < 0 \iff P_{00}(K) = 3(1-\beta)K^2 + 3\lambda K - (1-\beta)L > 0$ for all K. As with $P_0(K)$, $P_{00}(K)$ is a second degree polynomial in K with positive leading coefficient, therefore, it is positive if $(\boldsymbol{A_{1,(1-\beta)^2}}) : \Delta_{(1-\beta)^2} = 9\lambda^2 + 12(1-\beta)^2 L < 0$ and $(A_{2,(1-\beta)^2}) : -\frac{3}{4(1-\beta)}\lambda^2 - (1-\beta)L > 0$. We observe that when $L > 0$, then $\Delta_{(1-\beta)^2} > 0$ therefore $(\boldsymbol{A_{1,(1-\beta)^2}})$ is not possible.
Case 2: $L < 0$
Then $|T| - 1 - D < 0 \iff P_{000}(K) = 3(1+\beta)K^2 + 3\lambda K - (1+\beta)L > 0$ for all K. As with $P_0(K)$, $P_{000}(K)$ is a second degree polynomial in K with positive leading coefficient, therefore, it is positive if $(\boldsymbol{A_{1,(1+\beta)^2}}) : \Delta_{(1+\beta)^2} = 9\lambda^2 + 12(1+\beta)^2 L < 0$ and $(\boldsymbol{A_{2,(1+\beta)}}) : -\frac{3}{4(1+\beta)}\lambda^2 - (1+\beta)L > 0$. As above, we note that $(\boldsymbol{A_{1,(1+\beta)^2}})$ is satisfied only if $(\boldsymbol{A_{1,2,(1+\beta)^2}})$. To conclude, we note that $L = (\alpha-1)\mu_1 x^2 + \mu_2 x + 3\alpha < 0$ for all x if $\mu_1 < 0$ and $\delta = \mu_2^2 - 12(\alpha-1)\mu_1 < 0$ or for some x if $\mu_1 > 0$ and $\Delta > 0$. Obviously, if $\mu_1 < 0$, then $\Delta > 0$ making the first two of conditions impossible. Hence, one must have $\mu_1 > 0; \Delta > 0$ to expect $L < 0$ for some x.
We denote the condition $P_2 : \Delta > 0$. We can now state the stability theorem:

Theorem 5. *Let* $\mathbf{X}$ *be a fixed point of the DFHN model.*

(a) If $P_1(\beta), P_1(\beta+1)$ *and* P_2 *are satisfied, then* $\mathbf{X}$ *is asymptotically stable.*

(b) If one of $P_1(\beta), P_1(\beta+1)$*, or* P_2 *is not met, then* $\mathbf{X}$ *is unstable. In this case,* $\mathbf{X}$ *is either a saddle or a repeller.*

5 Qualitative analysis of the DFHN model

In the simulation below, we will illustrate the existence of equilibria and show that DFHN model preserves known phenomena of the CFHN, see for example [10]. For specifics, in Simulation 1 and 2, the starting points of the trajectories are respectively (3.5, 4) (red), (0.5, 4) (black), (-3.5, 2) (green), (0,-2) (magenta), (-3.5,-5) (cyan), and (3.5, -3) (blue).

5.1 Simulation 1: Existence of equilibria

Existence of equilibria for the CFHN or DFHN models depends on the discriminant function $\Delta = \Delta(a, \gamma, I)$ defined above. In this section, we represent the phase space diagrams of the

DFHN model when there is one asymptotically stable equilibrium point ($\Delta < 0$), one unstable equilibrium point ($\Delta = 0$), and three equilibrium points ($\Delta > 0$), among which two are asymptotically stable and one is unstable. In all figures, $\tau = 0.01$ and $\epsilon = 0.5$.

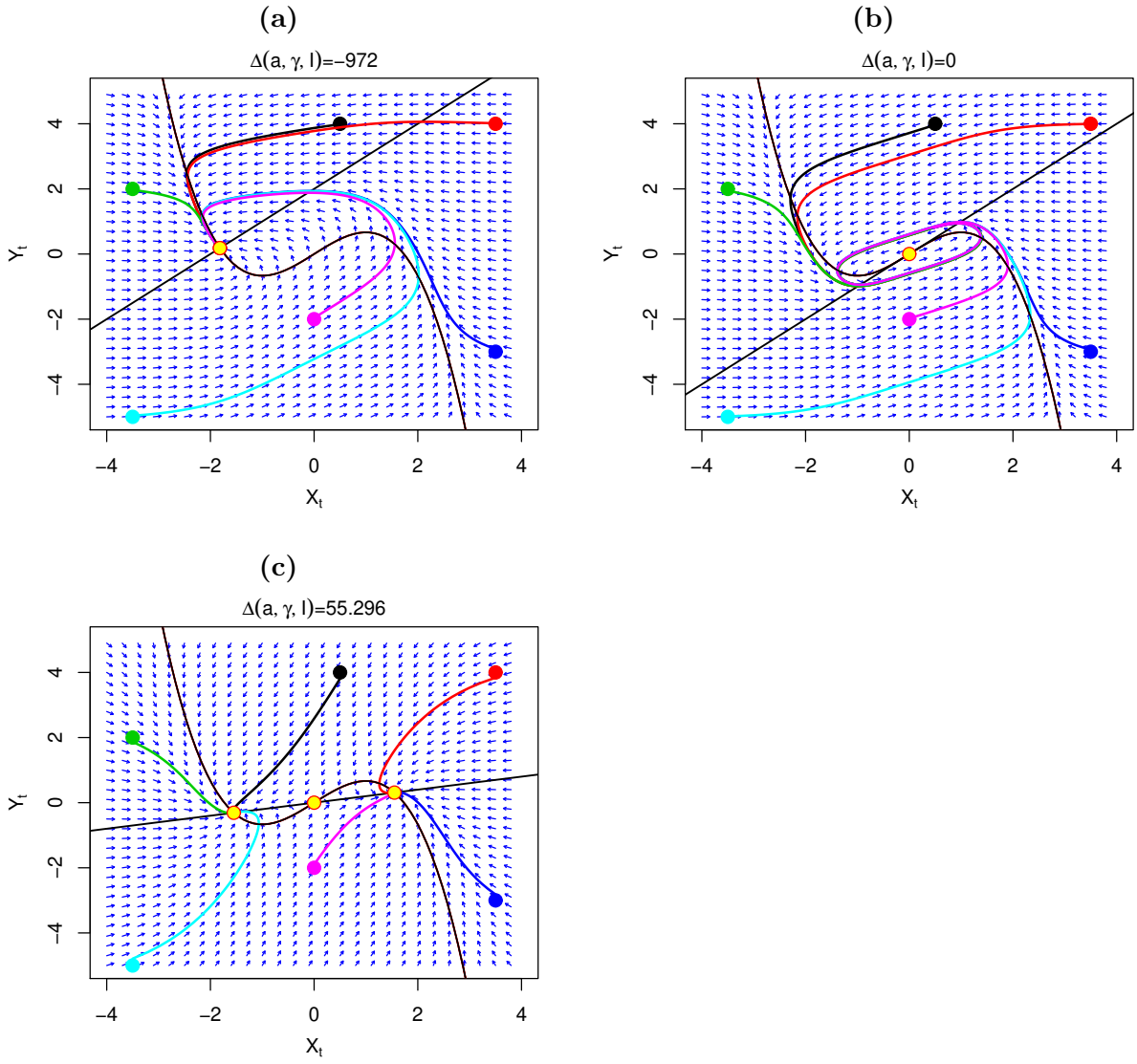

Figure 1: Figure 1**(a)** shows the case where $\Delta(a, \gamma, I) < 0$ and there is one stable equilibrium (yellow point). The parameters are $a = 2, \gamma = 1, I = 0$. Figure 1**(b)** shows the case where $\Delta(a, \gamma, I) = 0$ and there is one unstable equilibrium (yellow point). The parameters are $a = 0, \gamma = 1, I = 0$. Figure 1**(c)** shows the case where $\Delta(a, \gamma, I) > 0$ and there are three equilibria, two stable and one unstable (yellow points). The parameters are $a = 0, \gamma = 5, I = 0$ in all figures.

Figure 1**(a)** shows the resting state, that is, there is not enough stimulus in the system to create spikes. All trajectories, including the absolutely refractory ones (red and black), the relatively refractory (green), the self-excitatory (magenta and cyan), and the active trajectory (blue) eventually return to the resting state. In Figure 1**(b)**, as the stimulus is progressively increased, all trajectories are the result of spikes in the system, illustrated by a revolution around the intersection between the isoclines in equations (4.1) and (4.2). In Figure 1**(c)**,

eventually, with enough stimulus, there are two phenomena that occur. One is the excitation block phenomenon (see below) where spikes are blocked from occurring (blue, red, and magenta trajectories). This may occur with a large current I in the system as well. The second phenomenon is that of anodal block phenomenon where trajectories tend to make large excursions before being blocked from producing spikes. This may also occur when the current is negative and it is sometimes referred to as depolarization.

5.2 Simulation 2: Preservation of known phenomena

In this section, we will discuss known phenomena to the CFHN model. The CFHN model is known to have a phenomenon called *Absence of spikes or all-or-none-spikes* in a HH model. It also has phenomena known as the *spikes accommodation, the excitation block, and the break excitation phenomena*, see for instance [10]. We use the parameters $a = 0.97, \epsilon = 0.5, \gamma = 1$, and $\tau = 0.01$. Also, $I = 0.3$ (Figure 2), $I = 0.81$ (Figure 3), $I = 1$ (Figure 4), $I = 2.1$ (Figure 5), and $I = -1$ (Figure 6). In all phase space diagrams, the nullcline of x and y are respectively the black line and the black hyperbola. The red curve represents the nullcline of x, when by $I = 0$.

5.2.1 Absence of spikes phenomenon

The *absence of spikes phenomenon* is the fact that a small I results in a small amplitude-trajectory and a larger I results in a large amplitude-trajectory, producing a spike, see Figure 2 and Figure 3.

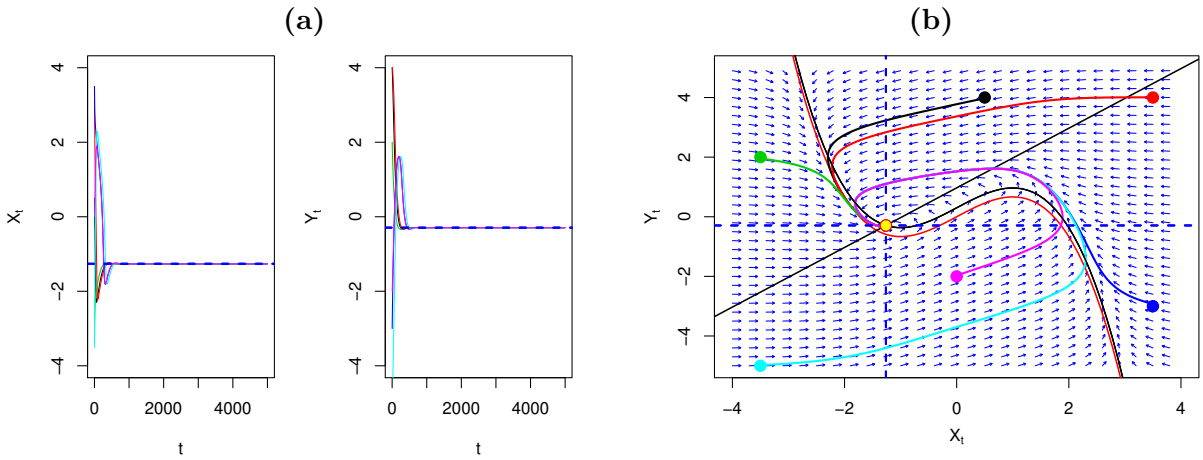

Figure 2: Here, $I = 0.3$. This stimulus is not strong enough to fire consistent spikes, Figure 2**(a)**. The system settles in an equilibrium whose coordinates are the only real solution of system of equations (4.1) and (4.2), and given as the intersection between the dashed blue lines, Figure 2**(b)**. This equilibria is classified as stable. This phase space diagram depicts the dynamics of the DFHN model.

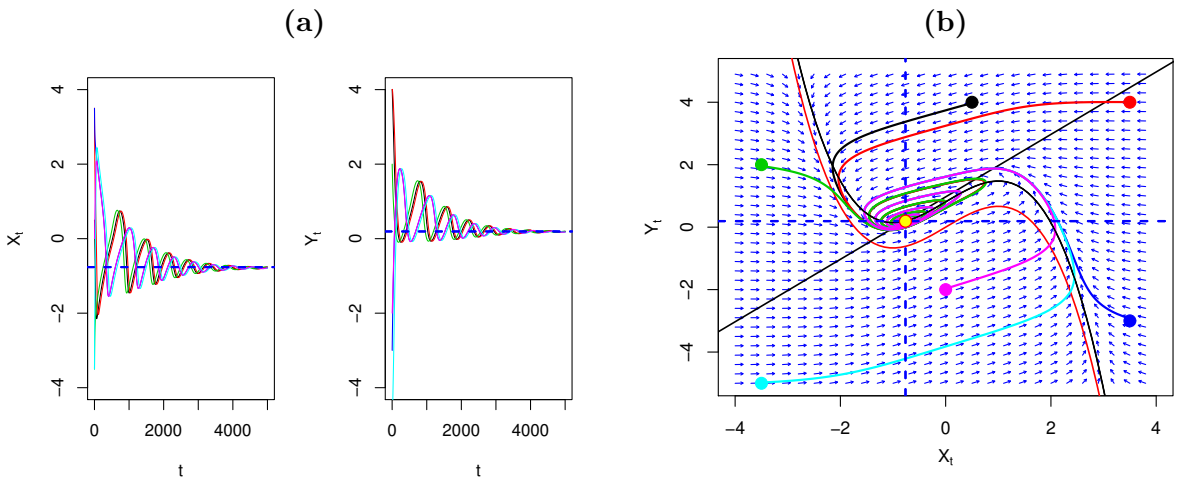

Figure 3: Here, $I = 0.81$. The stimulus is strong enough to produce spikes, Figure 3**(a)**, but not enough to sustain them over the long run, and the orbit settles in the fixed point classified as a spiral focus, Figure 3**(b)**.

5.2.2 Spikes accommodation phenomenon

The *spikes accommodation phenomenon* is the fact that repetitive spikes are produced as the network current or stimulus I increases beyond a certain threshold, see Figure 4.

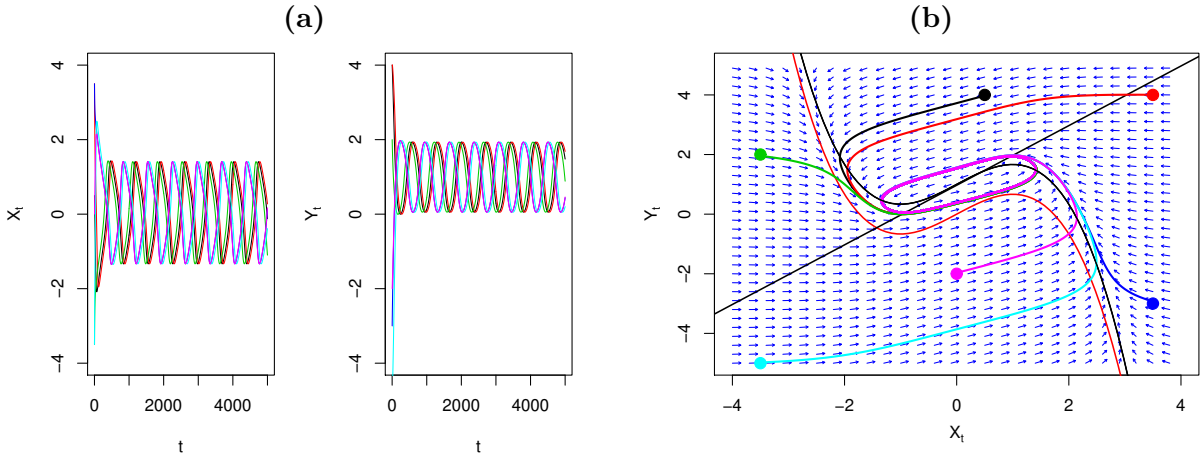

Figure 4: Here $I = 1$. The stimulus perturbs the stable equilibria into an unstable one, producing sustained spikes over the long run, Figure 4**(a)**. This is characterized by continuous rotations around the fixed point by all trajectories. The fixed point in this case is unstable, Figure 4**(b)**.

5.2.3 Excitation block phenomenon

The *excitation block phenomenon* is the fact that sustained spikes are blocked from occurring if large current I is input in the system, pushing the system to to settle in a stable equilibrium, see Figure 5.

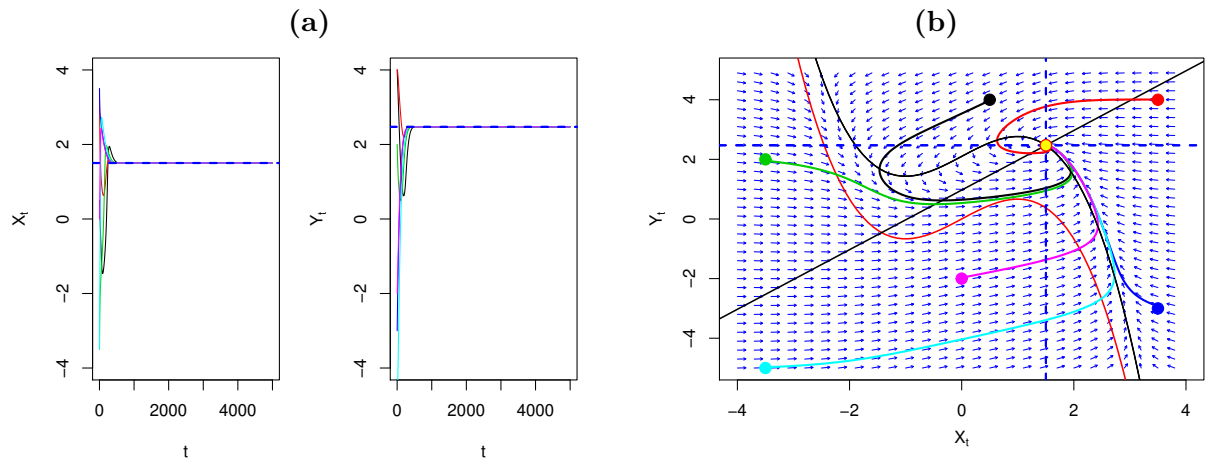

Figure 5: Here, $I = 2.1$. Sustained spikes are blocked from occurring, Figure 5**(a)**, and the unstable point becomes progressively a stable focus, Figure 5**(b)**.

5.2.4 Anodal break excitation

The *anodal break excitation phenomenon* is the fact that as the network current I becomes negative (hyperpolarization), a trajectory that starts below the resting states will make a large excursion in the phase space, firing a transient spike before returning to the resting state, see figure 6.

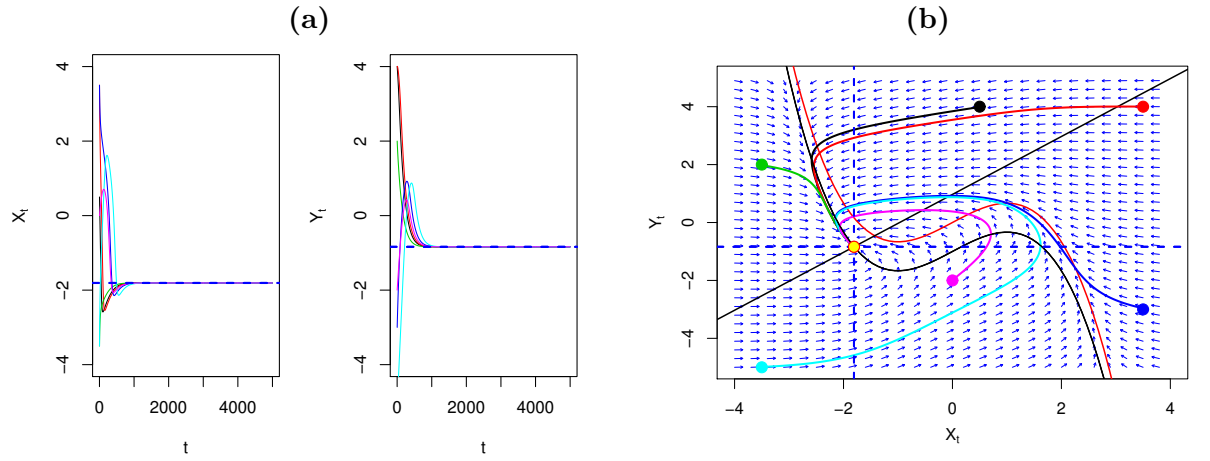

Figure 6: Here, $I = -1$. Any trajectory starting below the fixed point (cyan, magenta, and blue), takes a long excursion in the phase space, Figure 6**(b)**, firing a spike, before settling into the rest state.

6 Quantitative analysis

Now that we have shown that the main features of the CFHN model are preserved in the DFHN model, we will examine the DFHN model deeper. In oder to do so, we will use a distance-based similarity analysis of their times series and probability-based similarity (as in [6]) using the Wilcoxon-Rank-Sum test. We will also perform a sensitivity analysis to analyze the most influential parameters in the model.

6.1 Distance-based similarity analysis

In this section, we will discuss the similarity between the times series of the DFHN and CFHN models, using a distance measure. First, let $u = (u_1, u_2, \cdots, u_T)$ be vector in $\mathbb{R}^T$ where T is a positive integer. We define $\|u\| = \max_{1 \leq j \leq T} |u_j|$. We consider the following:

Definition 6. *Let $u = (u_1, u_2, \cdots, u_T)$, and $v = (v_1, v_2, \cdots, v_T)$ in $\mathbb{R}^T$.*
The similarity between u and v is defined as $S(u, v) = \frac{1}{1+\|u-v\|}$.
The dissimilarity between u and v is defined as $D(u, v) = 1 - S(u, v) = \frac{\|u-v\|}{1+\|u-v\|}$.

From this definition, we observe that: (1) $0 < S(u, v) \leq 1$ for all $u, v \in \mathbb{R}^T$. (2) If $u = v$, then $S(u, v) = 1$ and $D(u, v) = 0$ whereas if $\|u - v\| \to \infty$, then $S(u, v) \to 0$ and $D(u, v) \to 1$. For simplification purposes, let $S_x = S(x_t, x(t))$ and $D_x = D(x_t, x(t))$. S_y and D_y are defined similarly. Consider $x_0 = 0, y_0 = 1, \epsilon = 0.5, \gamma = 0.5, a = 1, I = 1$, and $T = 25$. Figure 7 represents the trajectory with initial point (x_0, y_0) in the xy-plane. The continuous red curve represents the CFHN and the discrete lines represent the DFHN model respectively for $\tau = 0.005, 0.01, \tau = 0.02$. We first note that the shape of the trajectory is the same for all values of τ. This is an illustration of the dynamical consistency of the NEDS method. Although initially the trajectories of the DFHN model are very close to that of the CFHN model, they we note that for larger values of τ, they differ while topologically being similar, see for instance Figure 13. A close inspection of the trajectories in Figure 7 shows that the continuous model has three loops with the largest being close to each other without being equal. The value of $\tau = 0.01$ seems to offer the trajectory most similar to this behavior. In general, τ has to be chosen using a reasonable criteria and noting that the NEDS requires τ to be reasonably small in the context of the variables, otherwise, it may be add bifurcations to the dynamics of the FHN model that did not exist before.

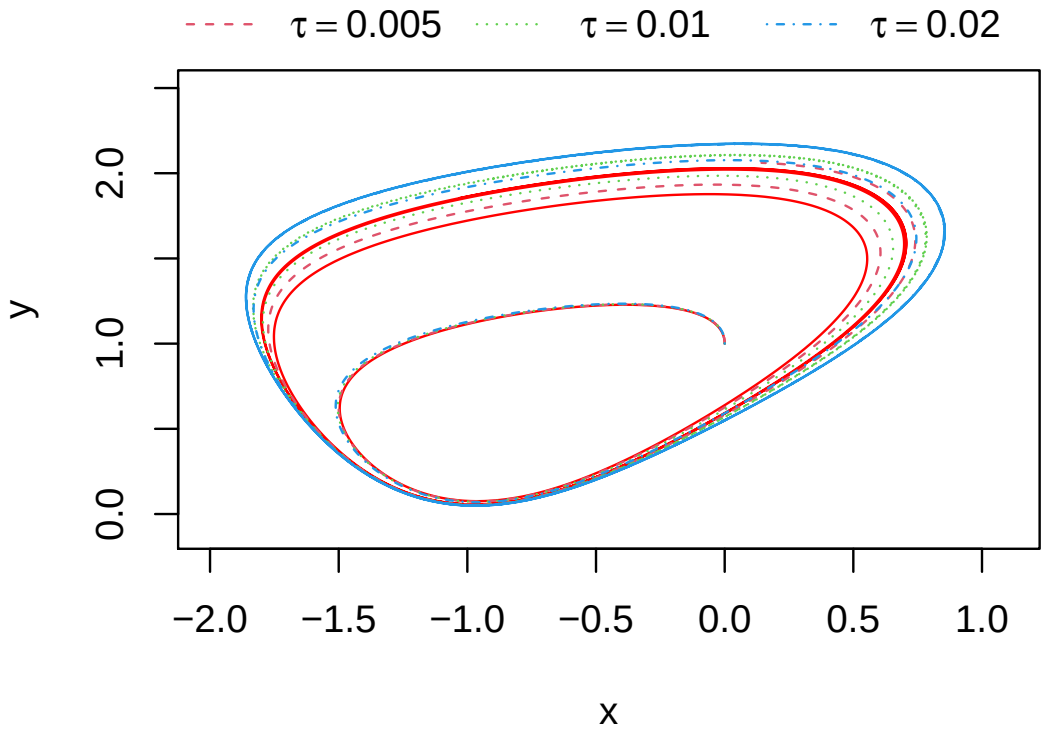

Figure 7: Trajectory of the CFHN model (red) and the DFHN model for $\tau = 0.005, 0.01, 0.02$ respectively

Now we analyze individual time series of the discrete and continuous models for the same parameters. Figure 8 represents the time series of the DFHN (blue) and CFHN (red), plotted for the parameter $\tau = 0.005, 0.01, 0.02$. A visual inspection shows that the two times series are very "similar" with similarity values $S_x = 0.9$ and $S_y = 0.5$ when $\tau = 0.01$. For $\tau = 0.005$, $S_x = 0.350$ and $S_y = 0.326$ and for $\tau = 0.02$, we have $S_x = 0.334$ and $S_y = 0.321$. In the last two cases, the difference is much more pronounced. Further, in Figure 9, we represent the changes of similarity and dissimilarity as a function of τ. We observe that for some small values of τ, the similarity is relatively high for both $x_t, x(t)$ and $y_t, y(t)$. The optimal value of τ seems to be 0.01. However, when τ increases, the similarity decreases and the dissimilarity increases. This can be explained by the fact that the combination of the parameters alters their importance, therefore, a proper scaling must be made.

(a)

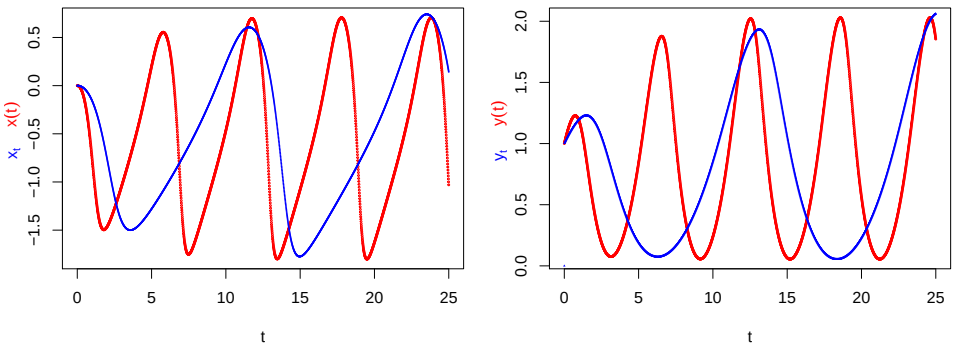

(b)

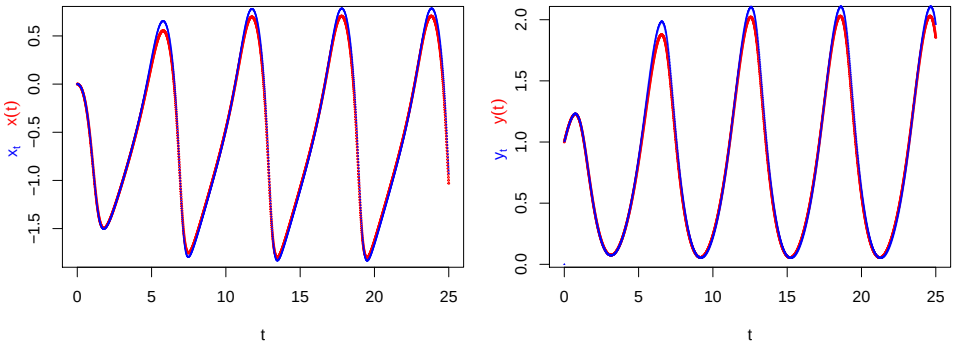

(c)

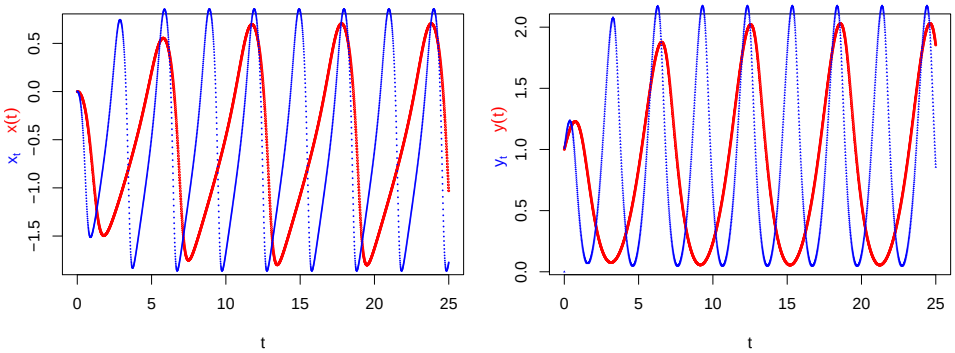

Figure 8: Times series for the CFHN model (red) and the DFHN model (blue) for $x_0 = 0, y_0 = 1, \epsilon = 0.5, \gamma = 0.5, a = 1, I = 1, T = 25$, and $\tau = 0.005$; see Figure 8**(a)**, $\tau = 0.01$; see Figure 8**(b)**, $\tau = 0.02$; see Figure 8**(c)**.

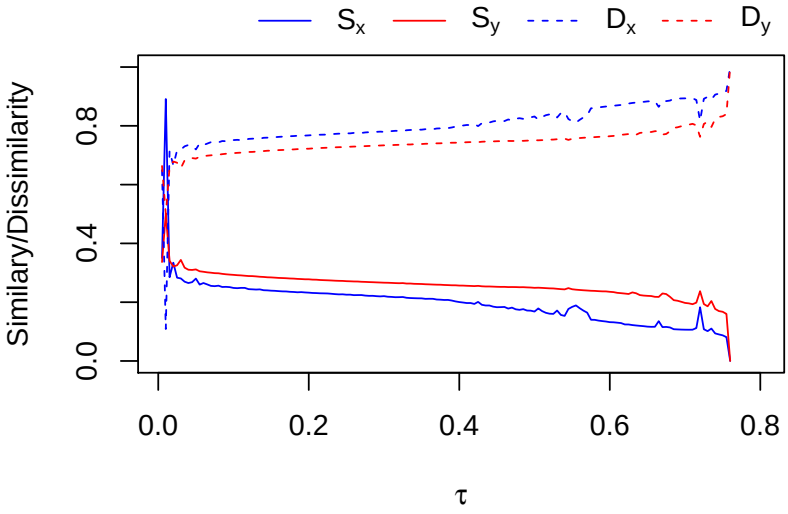

Figure 9: Similarity and dissimilarity measures for parameters $x_0 = 0, y_0 = 1, \epsilon = 0.5, \gamma = 0.5, a = 1, I = 1$, and $T = 25$.

6.2 Probability-based similarity analysis

Another way to compare the times series of the DFHN and CFHN models is to use a probability-based measure, such as a nonparametric test. To fix ideas, let us recall how the Wilcoxon-Mann-Whitney (WMW) Rank sum test works, see for instance [8] for further readings. Let U and V be two mutually independent random variables with respective cumulative distribution functions (c.d.f.) $F(u) = Pr(U \leq u)$ and $G(v) = Pr(V \leq v)$ for all $u, v \in \mathbb{R}$. Now consider random samples (independent and identically distributed) $U_1, U_2, \cdots, U_n$ and $V_1, V_2, \cdots, V_m$ from populations distributed similarly to U and V respectively. The WMW test has null hypothesis $H_0 : F(t) = G(t)$ for every $t \in \mathbb{R}$. This hypothesis suggests that U and $V$are identical (or have the same c.d.f. though not specified). The alternative hypothesis are $H_1 : G(t) = F(t - \Delta)$ for all $t \in \mathbb{R}$. $\Delta > 0$ means that V tends to produce values larger than that of U, $\Delta < 0$ means that V tends to produce values smaller than that of U. To make a decision based on samples collected, we will combine the $n + m$ sample values and compute $T_W = \sum_{j=1}^{m} Rank(V_j)$, where $Rank(V_j)$ is the rank or order of V_j in the combined sample. For large values of n and m, T_W is distributed like a Gaussian $N(\mu_W, \sigma_W^2)$ where $\mu_0 = 2^{-1}n(n + m + 1)$ and $\sigma_W^2 = 12^{-1}nm(n + m + 1)$. We will denote P.value_X as the p.value of the WMW test between x_t and $x(t)$. The similarity criteria will be that if the P.value_X is greater than 0.05 (standard practice in statistics), then x_t and $x(t)$ are similar, and the similarity increases as the P.value_X approaches 1. The same applies to P.value_Y. As above, we fix the parameters $x_0 = 0, y_0 = 1, \epsilon = 0.5, \gamma = 0.5, a = 1, I = 1$, and $T = 25$. In Figure 10, we observe that the P.value_X and P.value_Y are relatively large for $0 < \tau \leq 0.01$. This shows that x_t and $x(t)$ and y_t and $y(t)$ are statistically identical at significance level 0.05. However, x_t and $x(t)$ remain statistically identical for $0.01 \leq \tau < 0.45$ whereas y_t and $y(t)$ are not. This is at odds with the findings of section 6.1 where similarity or dissimilarity for x_t and $x(t)$ and that of y_t and $y(t)$ occurs for the same values of τ. This discrepancy can be explained by the fact that DFHN and CFHN models are coupled (or correlated) dynamical system of equations, and as such, the samples obtained are not independent as required in the WMW test, a similar caution already

raised in [6].

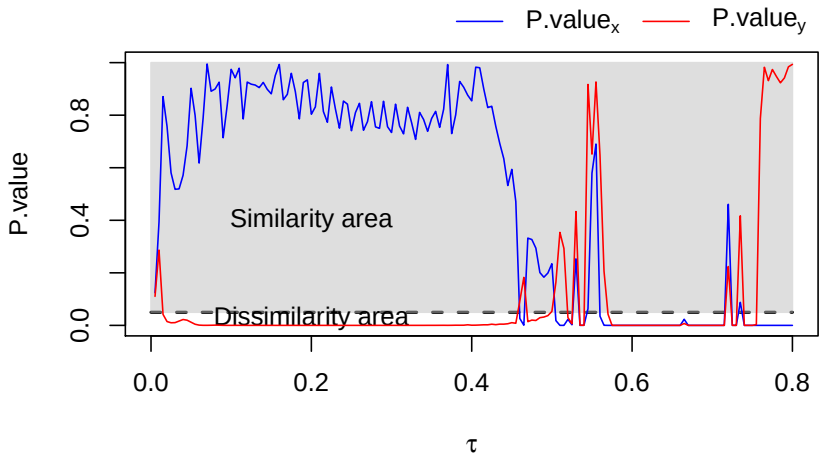

Figure 10: p.values of the WMW tests for $x_0 = 0, y_0 = 1, \epsilon = 0.5, \gamma = 0.5, a = 1, I = 1$, and $T = 25$.

6.3 Sensitivity Analysis

There are many approaches used in practice to perform sensitivity analysis each with advantages and inconveniences. The most popular methods are the so-called variance-based methods. To illustrate the approach, consider the following model:

$$R(t) = f(t, \alpha_1, \alpha_2, \cdots, \alpha_d), \tag{6.1}$$

where $R(t)$ is an output or a response at time t to d factors α_i for $1 \leq i \leq d$. Assuming uncertainty (stochasticity) in the factors α_i, let the total variance of $R(t)$ be defined as $V(t) = \text{Var}(R(t))$. Then we have the following decomposition of the variance of $R(t)$:

$$V(t) = \sum_{i=1}^{d} V_i(t) + \sum_{i=1}^{d-1} \sum_{j=i+1}^{d} V_{ij}(t) + \sum_{i=1}^{d-2} \sum_{i=j+1}^{d-1} \sum_{k=1}^{d} V_{ijk}(t) + \cdot + V_{1\cdots d}(t), \tag{6.2}$$

where $V_i(t) = \text{Var}(E[R(t)|\alpha_i])$ is the variability associated with the main effect α_i, $V_{ij}(t) = \text{Var}(E[R(t)|\alpha_i, \alpha_j]) - V_i(t) - V_j(t)$ is the variability associated with the interaction between α_i and α_j, $V_{ijk}(t) = \text{Var}(E[R(t)|\alpha_i, \alpha_j, \alpha_k]) - V_i(t) - V_j(t) - V_k(t) - V_{ij}(t) - V_{ik}(t) - V_{jk}(t)$ is the variability associated with the interaction between α_i, α_j, and α_k, etc, and $E[R(t)|\alpha_i]$ is the expected value of $R(t)$ given α_i. We note that $X|Y$ here means X given Y(or X conditioned on Y). We define the first, second, third order sensitivity indices as:

$$S_i(t) = \frac{V_i(t)}{V(t)}, \; S_{ij}(t) = \frac{V_{ij}(t)}{V(t)}, \; S_{ijk}(t) = \frac{V_{ijk}(t)}{V(t)} \; .$$

We will also be interested in total-order effect sensitivity index $T_{S_i}(t)$ which is the sum over first order effect of the ith factor and its interactions of any order with other factors, that is,

$$T_{S_i}(t) = S_i(t) + S_{ij}(t) + S_{ijk}(t) + \cdots + S_{i\cdots d}(t) = S_i(t) + \sum_{l=1}^{d} S_{ij_1j_2\cdots j_l}(t) \; .$$

For implementation, we will use the so-called "fast99" method, which allows to estimate the Sobol's first and total indices (see [20]) with the so-called "Saltelli extended-FAST" method, see [18]. The implementation was carried out in R (4.00 version) using the packages *sensitivity* and *multisensi*. For the DFHN model, the factors of interest are starting point (x_0, y_0), and the model parameters $\tau, \epsilon, \gamma, a$, and I, so that $d = 7$. We will use $T = 5$ to better visualize the evolution of the sensitivity indices (The case $T = 100$ is given in the appendix B). The seven parameters were taken from the hypercube $[-4, 4] \times [-4, 4] \times [0.05, 2] \times [0.05, 2] \times [0.1, 2] \times [0.05, 5] \times [-5, 5]$.

From Figure 11, we observe that, in terms of variance, x_0 is the most important parameter at $t1$ for both x_t and y_t. At t2, I becomes the most important parameter for x_t whereas γ is the one for y_t. γ remains the most important parameter afterward with a total index close to 0.9. We observe that the other parameters have rising total indices overtime and eventually, they will have equal importance overtime, see Figure 14 in Appendix B. This can be explained by the fact that the total index contains all various interactions with other parameters and the influence of those interactions increases overtime as seen in Figure 14. That parameters I, x_0, y_0, and ϵ are the most influential for x_t in the beginning. However, the influence of ϵ decreases overtime, see Figure 14**(a)**. This is confirmation that the discrete model performs as expected since these are the only parameters involved in that the model. We observe also that parameters a, γ and τ have less influence on the variance early on but overtime, a becomes very influential. The same observation can be made about parameters γ, a, x_0, y_0 and τ which are the most important for y_t early on. Overtime, the most influential parameters for y_t are γ, a, x_0, y_0 and I, see Figure 14**(b)** .
These findings are further confirmed in Figure 12. Indeed, we show the evolution of first order indices (light gray) relative to the total index (black) for x_t (Figure 12**(a)**) and for y_{t+1} (Figure 12**(b)**). Figure 12**(b)** reveals in particular that the first order sensitivity of parameter γ remains an important part of the total sensitivity index overtime while Figure 12**(a)** reveals that the contribution of the first order sensitivity index of ϵ in its total sensitivity index decreases overtime. This means that interactions between the parameters overtime are the main sources of variability for of x_t whereas for y_t, γ is still a great source of variability. The takeaway from this dynamic sensitivity analysis is that there is no unexplained part of the variance, that is, no exogenous quantity contributes to the variance overtime.

Remark 7. *Of interest in sensitivity analysis is also the notion of "generalized sensitivity index" (GSI). However, there is no unifying quantity that has emerged in the literature about the best way to assess the GSI for a model. We therefore chose in this paper not to include it in our discussion.*

x_t y_t

(a) **(b)**

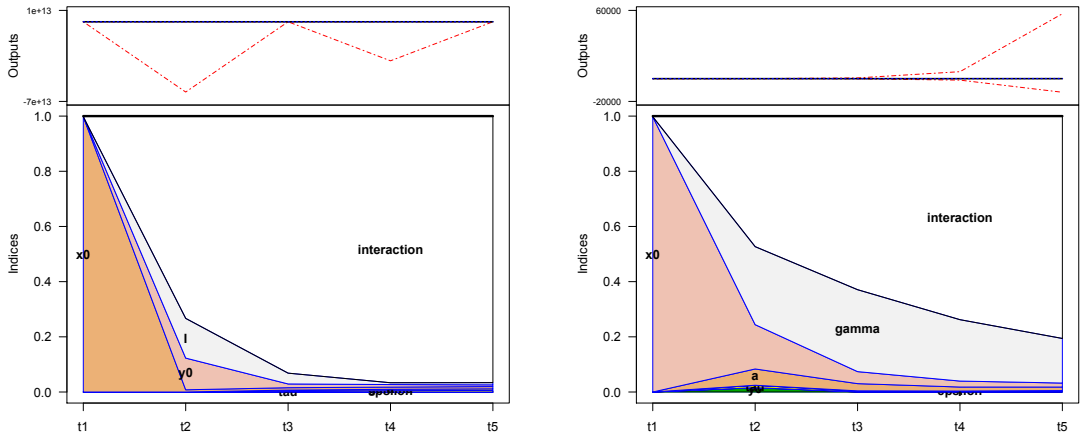

(c) **(d)**

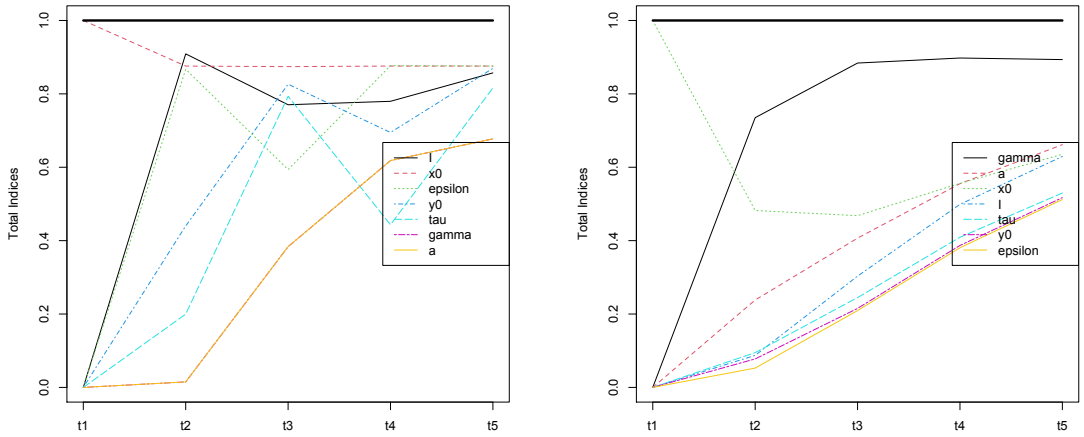

Figure 11: **(a)** and **(b)** show the evolution of first indices and **(c)** and **(d)** show the evolution of total indices from t1 to t5 for outputs x_t and y_t.

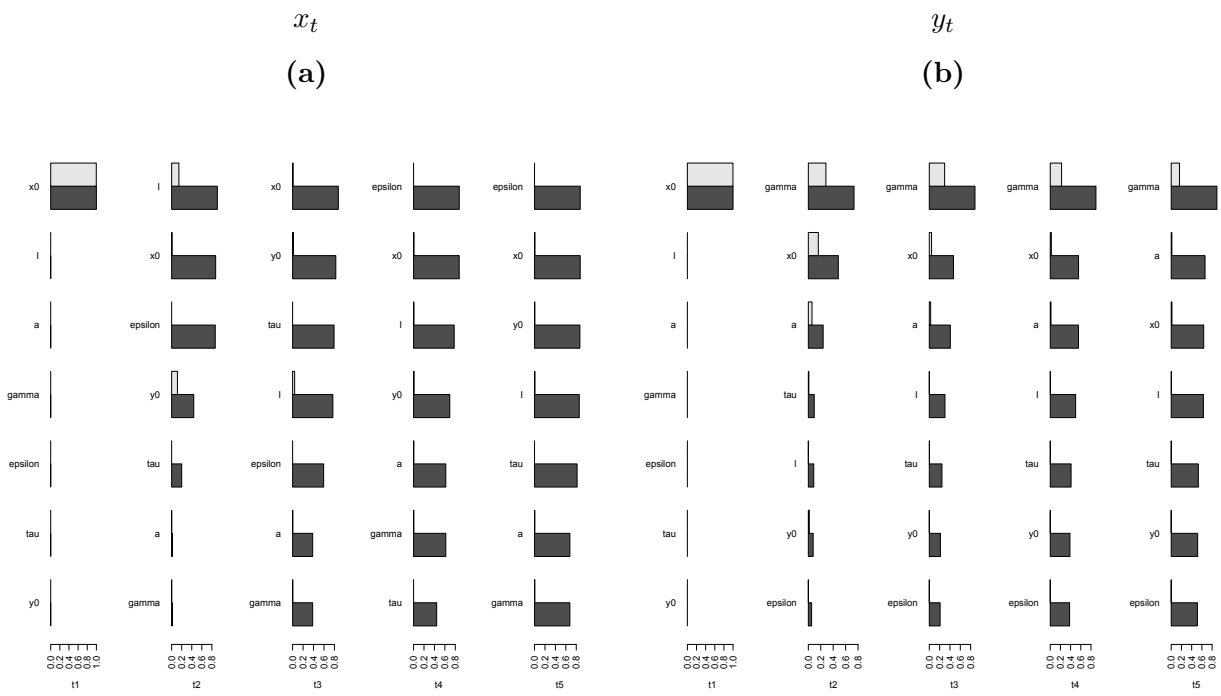

Figure 12: Figure 12**(a)** and Figure 12**(b)** show the evolution of first order indices (light gray) relative to the total index (black) for x_t and for y_t.

7 Concluding remarks

In this paper, we have proposed a discrete version of the FitzHugh-Nagumo model using a NEDS method, an iteration of the non-standard discretization technique of Mickens [15]. Advantages of the model obtained include the fact that it faithfully reproduces the behavior of the ODE it was discretized from, preserving the original dynamics, and without adding behaviors that would have otherwise not existed. Often, DE models obtained using the Euler method would have mathematical properties not present in the ODE. One disadvantage of the method is that the stability analysis of the discrete system is not easy to discuss and the conditions on the parameters to obtain stability of the fixed points are not trivial, even after reparametrization. This is an improvement that may warrant further discussions. The simplicity of the discrete model may make it useful in parameter estimation in data analysis. Indeed, experimental data and parameter estimation from these data on the FHN model have been attempted. However, it was not always clear how the parameters were estimated from data, see for example [5]. This model could be used to improve the values of the parameters obtained during that experiment.

References

[1] S. N. Elaydi, *Discrete Chaos*, Chapman & Hall/CRC, 2007.

[2] C. E. Elmer and E. S. Van Vleck, *Spatially discete fitzhugh- nagumo equations*, SIAM J. Appl. Math., 65 (2005), pp. 1153–1174.

[3] R. FitzHugh, *Impulses and physiological states in theoretical models of nerve membrane*, Biophysical Journal, 1 (1961), pp. 445–466.

[4] M. Foroutan, J. Manafian, and . Taghipour-Farshi, *Exact solutions for fitzhugh–nagumo model of nerve excitation via kudryashov method*, Opt. Quant. Electron., 49 (2017).

[5] J. P. A. Foweraker, D. Brown, and R. W. Marrs, *Discrete-time stimulation of the oscillatory and excitable forms of a fitzhugh–nagumo model applied to the pulsatile release of luteinizing hormone releasing hormone*, Chaos: An Interdisciplinary J. of Non. Sc., 5 (1995), pp. 200–208.

[6] F. Grassetti, M. Gusowska, and E. Michetti, *A dynamically consistent discretization method for goodwin model*, Chaos, Solitons, and Fractals, 130 (2020). Article 107627.

[7] A. L. Hodgkin and A. F. Huxley, *A quantitative description of membrane currents and its application to conduction and excitation in nerve*, J. Physiol., 117 (1952).

[8] M. Hollander and D. A. Wolfe, *Nonparametric statistical methods*, John Wiley & Sons, New York-London-Sydney, 1999. Wiley Series in Probability and Mathematical Statistics.

[9] H. J. Hupkes and B. Sandstede, *Traveling pulses for the discrete fitzhugh-nagumo system*, SIAM J. Appl. Math, 9 (2010), pp. 827–882.

[10] E. M. Izhikevich, *Dynamical Systems in Neuroscience: The Geometry of Excitability and Bursting*, The MIT Press, Cambridge, MA, 2007.

[11] Z. Jing, Y. Chang, and B. Guo, *Bifurcation and chaos in discrete fitzhugh–nagumo system*, Chaos, solitons, and fractals, 21 (2004), pp. 701–720.

[12] N. A. Kudryashov, *Asymptotic and exact solutions of the fitzhugh–nagumo model*, Regular and Chaotic dynamics, 23 (2018), pp. 152–160.

[13] N. A. Kudryashov, R. B. Rybka, and A. G. Sboev, *Analytical properties of the perturbed fitzhugh–nagumo model*, Applied Mathematics Letters, 76 (2018), pp. 142–147.

[14] E. Kwessi, S. Elaydi, B. Dennis, and G. Livadiotis, *Nearly exact discretization of single species population models*, Natural Resource Modeling, (2018).

[15] R. E. Mickens, *Advances in the applications of nonstandard finite diffference scheme*, Hackensack, NJ : World Scientific, 2005.

[16] ——, *Difference equations: Theory, applications, and advanced topics*, Monographs and Research Notes in Mathematics, CRC Press, Boca Raton, FL, xxii+553, third ed., 2015.

[17] J. Nagumo, S. Arimoto, and S. Yoshizawa, *An active pulse transmission line simulating nerve axon*, Proceedings of the IRE, 50 (1962), pp. 2061–2070.

[18] A. Saltelli, S. Tarantola, and K.-S. Chan, *A quantitative model-independent method for global sensitivity analysis of model output*, Technometrics, 41 (1999), pp. 39–56.

[19] S. Sehgal and A. J. Foulkes, *Numerical analysis of subcritical hopf bifurcations in the two-dimensional fitzhugh-nagumo model*, Physical Review E, 102 (2020), p. 012212.

[20] I. M. Sobol, *Sensitivity estimates for nonlinear mathematical models*, Mat. Modelirovanie, 2 (1990), pp. 112–118.

Appendix

Appendix A: Supplemental Figures for similarity analysis

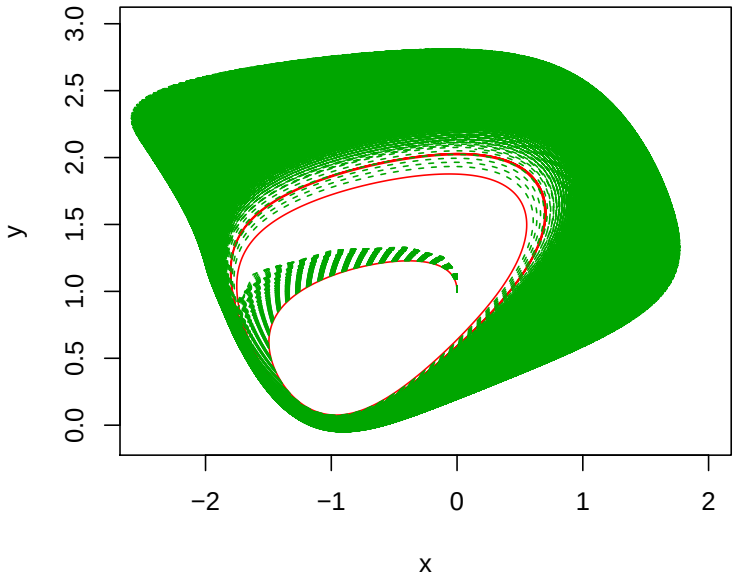

Figure 13: This figure shows the trajectory (red) of the CFHN model for parameters $x_0 = 0, y_0 = 1, \epsilon = 0.5, \gamma = 0.5, a = 1, I = 1$, and $T = 25$. The green dashed lines represent the trajectories of the DFHN for the same parameters and for 100 values of τ, equally spaced between 0.005 and 0.3.

Appendix B: Supplemental Figures for sensitivity analysis

x_{t+1} **(a)** y_{t+1} **(b)**

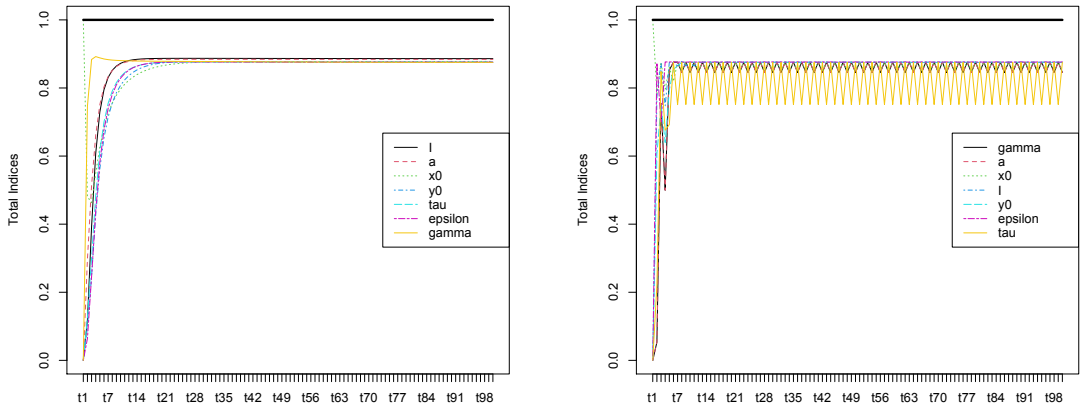

Figure 14: Figure 14**(a)** and Figure 14**(b)** show the evolution of total indices from t1 to t100 for outputs x_{t+1} and y_{t+1}.